

EF Cha: Warm Dust Orbiting a Nearby 10 Myr Old Star

Joseph H. Rhee¹, Inseok Song², B. Zuckerman³

ABSTRACT

Most Vega-like stars have far-infrared excess ($60\,\mu\text{m}$ or longward in *IRAS*, *ISO*, or *Spitzer MIPS* bands) and contain cold dust ($\lesssim 150\,\text{K}$) analogous to the Sun’s Kuiper-Belt region. However, dust in a region more akin to our asteroid belt and thus relevant to the terrestrial planet building process is warm and produces excess emission in mid-infrared wavelengths. By cross-correlating Hipparcos dwarfs with the MSX catalog, we found that EF Cha, a member of the recently identified, $\sim 10\,\text{Myr}$ old, “Cha-Near” Moving Group, possesses prominent mid-infrared excess. N-band spectroscopy reveals a strong emission feature characterized by a mixture of small, warm, amorphous and possibly crystalline silicate grains. Survival time of warm dust grains around this A9 star is $\lesssim 10^5$ yrs, much less than the age of the star. Thus, grains in this extra-solar terrestrial planetary zone must be of “second generation” and not a remnant of primordial dust and are suggestive of substantial planet formation activity. Such second generation warm excess occurs around $\sim 13\%$ of the early-type stars in nearby young stellar associations.

Subject headings: circumstellar matter — infrared: stars — planetary systems: protoplanetary disks — stars: individual (EF Cha)

1. Introduction

In our Solar System, zodiacal dust grains are warm ($\gtrsim 150\,\text{K}$) and found within $\sim 3\,\text{AU}$ of the Sun. Slow but persistent collisions between asteroids complemented by material released from comets now replenish these particles. Similar warm dust particles around other stars are also expected and would be manifested as excess mid-infrared emission.

¹Gemini Observatory, 670 North A’ohoku Place, Hilo, HI 96720; current address (Department of Physics and Astronomy, Box 951547, University of California, Los Angeles, CA 90095-1562; rhee@astro.ucla.edu)

²Gemini Observatory, 670 North A’ohoku Place, Hilo, HI 96720

³Department of Physics and Astronomy, Box 951547, University of California, Los Angeles, CA 90095-1562; NASA Astrobiology Institute

The implication of “warm” excess stars for the terrestrial planet-building process has prompted many searches including several pointed observing campaigns with *Spitzer* (Gorlova et al. 2004; Rieke et al. 2005; Low et al. 2005; Beichman et al. 2005, 2006; Bryden et al. 2006; Hines et al. 2006; Gorlova et al. 2006; Smith et al. 2006). However, a lack of consensus of what constitutes a “warm excess” has resulted in ambiguity and some confusion in the field. For example, *Spitzer* surveys with MIPS revealed a number of stars with excess emission in the $24\mu\text{m}$ band. However, very few of these may turn out as genuine “warm excess” stars because the detected $24\mu\text{m}$ emission is mostly the Wien tail of emission from cold ($T < 150\text{ K}$) dust grains (Rhee et al. 2007).

For black-body grains, $T_{\text{dust}} = T_*(R_*/(2R_{\text{dust}}))^{1/2}$, where R_{dust} is the distance of a grain from a star of radius R_* and temperature T_* . Due to the dependence of T_{dust} on T_* and R_* , the terrestrial planetary zone (TPZ) around high mass stars extends further out than that around low mass stars. Therefore, R_{dust} is not a good way to define the TPZ while dust equilibrium temperature is equally applicable to all main-sequence stars. In our Solar system, T_{dust} is 150K near the outer boundary of the asteroid belt ($\sim 3.5\text{ AU}$), and the zodiacal dust particles are sufficiently large ($\sim 30\mu\text{m}$) that they do radiate like blackbodies. To specify a TPZ independent of the mass of the central star, we define the TPZ to be the region where $T_{\text{dust}} \gtrsim 150\text{ K}$. Then an A0 star has 25 AU and an M0 star has 0.9 AU as the outer boundary of their TPZ. Because of the way it is defined, TPZ applies only to the location of grains that radiate like a blackbody.

According to the *Spitzer* surveys listed above, the presence of dust in the TPZ characterized by excess in the mid-IR is quite rare for stars $\gtrsim 10\text{ Myrs}$ old. For ages in the range of 8–30 Myr, a posited period of the terrestrial planet formation in our Solar System, only a few stars appear to possess warm dust according to our analysis (see § 5 and Table 1): $\eta\text{ Cha}$, a B8 member of 8 Myr old $\eta\text{ Cha}$ cluster (Mamajek et al. 1999), $\eta\text{ Tel}$ & HD 172555, A0- and A7-type members of the 12 Myr old $\beta\text{ Pic}$ moving group (Zuckerman & Song 2004), HD 3003, an A0 member of the 30 Myr old Tucana/Horologium moving group (Zuckerman et al. 2001), and HD 113766, an F3 binary star ($1.2''$ separation, Dommange & Nys 1994), in the Lower Centaurus Crux (LCC) Association (Chen et al. 2005).

In this paper, we present the A9 star EF Cha, another example of this rare group of stars with warm dust at the epoch of terrestrial planet formation.

2. MSX Search for Mid-IR Excess Stars

Hipparcos, 2MASS and Mid Course Experiment (MSX, Egan et al. 2003) sources were cross-correlated to identify main-sequence stars with excess emission at mid-IR wavelengths. Out of $\sim 68,000$ Hipparcos dwarfs with $M_V \geq 6.0(B - V) - 2.0$ (see Rhee et al. 2007 for an explanation of this M_V constraint) in a search radius of $10''$, ~ 1000 stars within 120 pc of Earth were identified with potential MSX counterparts.

Spectral Energy Distributions (SED) were created for all $\sim 1,000$ MSX identified Hipparcos dwarfs. Observed fluxes from Tycho-2 B_T and V_T and 2MASS J , H , and K_s , were fit to a stellar atmospheric model (Hauschildt et al. 1999) via a χ^2 minimization method (see Rhee et al. 2007, for detailed description of SED fitting). From these SED fits, about 100 Hipparcos dwarfs were retained that showed apparent excess emission in the MSX $8\mu\text{m}$ band (that is, the ratio [MSX flux - photosphere flux] / MSX flux uncertainty must be > 3.0). Since a typical positional 3σ uncertainty of MSX is $\sim 6''$ (Clarke et al. 2005) and MSX surveyed the Galactic plane, a careful background check is required to eliminate contamination sources. By over-plotting the 2MASS sources on the Digital Sky Survey (DSS) images, we eliminated more than half of the apparent excess stars that included any dubious object (i.e., extended objects, extremely red objects, etc.) within a $10''$ radius from the star. Among the stars that passed this visual check, EF Cha was selected for follow-up observations at the Gemini South Telescope. Independent IRAS detections at 12 and $25\mu\text{m}$ made EF Cha one of the best candidates for further investigation.

3. Ground-based Follow-up Observations & MIPS Photometry

An N-band image and a spectrum of EF Cha were obtained using the Thermal-Region Camera Spectrograph (T-ReCS) at the Gemini South Telescope in March and July of 2006 (GS-2006A-Q-10), respectively. Thanks to the queue observing mode at Gemini Observatory, the data were obtained under good seeing and photometric conditions. The standard “beam switching” mode was used in all observations in order to suppress sky emission and radiation from the telescope. Data were obtained chopping the secondary at a frequency of 2.7 Hz and nodding the telescope every ~ 30 sec. Chopping and nodding were set to the same direction, parallel to the slit for spectroscopy.

Standard data reduction procedures were carried out to reduce the image and the spectrum of EF Cha at N-band. Raw images were first sky-subtracted using the sky frame from each chop pair. Bad pixels were replaced by the median of their neighboring pixels. Aperture photometry was performed with a radius of 9 pixels ($0.9''$) and sky annuli of 14 to

20 pixels. The spectrum of a standard star (HD 129078) was divided by a Planck function with the star’s effective temperature (4500K) and this ratioed spectrum was then divided into the spectrum of EF Cha to remove telluric and instrumental features. The wavelength calibration was performed using atmospheric transition lines from an unchopped raw frame. The 1-D spectrum was extracted by weighted averaging of 17 rows.

For the N-band imaging photometry, the on-source integration time of 130 seconds produced $S/N > 30$ with $FWHM \sim 0.54''$. For the N-band spectrum, a 886 second on-source exposure resulted in $S/N > 20$. A standard star, HIP 57092, was observed close in time and position to our target and was used for flux calibration of the N-band image of EF Cha. For spectroscopy, HD 129078, a KIII 2.5 star, was observed after EF Cha at a similar airmass and served as a telluric standard.

While our paper was being reviewed, Spitzer Multiband Imaging Photometer for Spitzer (MIPS) archival images of EF Cha at 24 and $70\mu\text{m}$ were released from the Gould’s Belt Legacy program led by Lori Allen. EF Cha was detected at MIPS 24 μm band but not at MIPS 70 μm band. We performed aperture photometry for EF Cha at 24 μm on the post-BCD image produced by Spitzer Science Center MIPS pipeline. We used aperture correction of 1.167 for the 24 μm image given at the SSC MIPS website (<http://ssc.spitzer.caltech.edu/mips/apercorr/>) with aperture radius of $13''$ and sky inner and outer annuli of $20''$ and $32''$, respectively. For MIPS 70 μm data, we estimated 3σ upper limits to the non-detection on the mosaic image that we produced using MOPEX software on BCD images.

4. Results

Table 2 lists the mid-IR measurements of EF Cha from MSX, IRAS, MIPS, and Gemini T-ReCS observations. The T-ReCS N-band image (FOV of $28.8'' \times 21.6''$) confirmed that no other mid-IR source appears in the vicinity of EF Cha and that the mid-IR excess detected by the space observatories (IRAS & MSX) originates solely from EF Cha. A strong silicate emission feature in the N-band spectrum (Figure 1) indicates the presence of warm, small ($a \lesssim 5\mu\text{m}$, see Figure 6 in Rhee & Larkin 2006) dust particles. Amorphous silicate grains dominate the observed emission feature. However, crystalline silicate structure, probably forsterite, appears as a small bump near $11.3\mu\text{m}$ (Kessler-Silacci et al. 2006). Polycyclic Aromatic Hydrocarbon (PAH) particles can also produce an emission feature at $11.3\mu\text{m}$. However, absence of other strong PAH emission features at 7.7 and $8.6\mu\text{m}$ indicates that the weak $11.3\mu\text{m}$ feature does not arise from PAHs. Furthermore, although PAH particles do appear in some very young stellar systems, they have not been detected around stars as old as 10 Myr. In contrast, crystalline silicates such as olivine, forsterite, etc. are seen in a few

such stellar systems (Song et al. 2005; Schuetz et al. 2005; Beichman et al. 2006; Lisse et al. 2006).

The dust continuum excess of EF Cha was fit with a single temperature blackbody curve at 240 K by matching the flux density at $13\,\mu\text{m}$ and the MIPS $70\,\mu\text{m}$ upper limit (Figure 1). The $3\,\sigma$ upper limit at MIPS $70\,\mu\text{m}$ band indicates that the dust temperature should not be colder than 240K. Figure 1 shows that MIPS $24\,\mu\text{m}$ flux is $\sim 30\,\text{mJy}$ lower than IRAS $25\,\mu\text{m}$ flux. Due to the small MIPS aperture size compared with IRAS, MIPS $24\,\mu\text{m}$ flux often comes out smaller when nearby contaminating sources are included in the large IRAS beam. The ground-based T-ReCS ($28.8'' \times 21.6''$) image of EF Cha at N-band, however, shows no contaminating source in the vicinity of EF Cha. Thus, the higher flux density at IRAS $25\,\mu\text{m}$ perhaps indicates the presence of a significant silicate emission feature near $18\,\mu\text{m}$ included in the wide passband of the IRAS $25\,\mu\text{m}$ filter ($18.5 - 29.8\,\mu\text{m}$). A recent Spitzer IRS observation of another warm excess star, BD+20 307 (Song et al. 2005), shows a similar discrepancy between the IRAS $25\,\mu\text{m}$ flux and MIPS $24\,\mu\text{m}$ flux in the presence of a significant silicate emission feature at $\sim 18\,\mu\text{m}$ (Weinberger et al. 2007 in preparation), consistent with our interpretation. MIPS $24\,\mu\text{m}$ flux is slightly above our 240 K dust continuum fit. The wide red wing of an $18\,\mu\text{m}$ silicate emission feature could contribute to a slight increase in MIPS $24\,\mu\text{m}$ flux.

5. Discussion

5.1. Debris Disk Characteristics of EF Cha

EF Cha was detected in the ROSAT X-ray All Sky Survey with $L_x/L_{bol} = 10^{-4.68}$ which suggests a very young age for an A9 star (see Figure 4 in Zuckerman & Song 2004). On the basis of this X-ray measurement, Hipparcos distance (106 pc), location in the sky (RA = $12^\circ 07'$, Dec = -79°), and proper motion (pmRA = -40.2 ± 1.2 & pmDE = -8.4 ± 1.3 in mas/yr), EF Cha is believed to be a member of the “Cha-Near” moving group (avg. RA = $12^\circ 00'$ & avg. DEC = -79° , avg. pmRA = -41.13 ± 1.3 & avg. pmDEC = -3.32 ± 0.86 in mas/yr, Zuckerman & Song 2004; Zuckerman et al. 2007), which is ~ 10 Myr old and typically $\sim 90\text{pc}$ from Earth.

Large blackbody grains in thermal equilibrium at 240 K, would be located ~ 4.3 AU from EF Cha while small grains, especially those responsible for the silicate emission features in our N-band spectrum, radiate less efficiently and could be located at > 4.3 AU. Recent Spitzer MIPS observations confirmed that all aforementioned (§ 1) warm excess stars do not have a cold dust population, indicating few large grains at large distances (Chen et al. 2006;

Smith et al. 2006). Lack of cold large grains, in turn, suggests local origin of the small grains seen in these warm excess stars. Without cold excess from Spitzer MIPS $70\,\mu\text{m}$ data, small grains in EF Cha should originate in the TPZ, probably by the breakup of large grains in the TPZ, rather than inward migration from an outer disk. Even in the unlikely event that silicate emission comes from small grains in an outer disk that were blown away by radiation pressure as in Vega (Su et al. 2005), the dominant carrier of 240 K continuum emission would still be large grains (Aigen Li 2007, private communication).

The fraction of the stellar luminosity reradiated by dust, τ , is $\sim 10^{-3}$, which was obtained by dividing the infrared excess between $7\,\mu\text{m}$ and $60\,\mu\text{m}$ by the bolometric stellar luminosity. This τ is $\sim 10,000$ times larger than that of the current Sun’s zodiacal cloud ($\sim 10^{-7}$) but appears to be moderate for known debris disk systems at similar ages (see Figure 4 in Rhee et al. 2007). Rhee et al. (2007) show that the ratio of dust mass to τ of a debris system is proportional to the inverse-square of dust particle semimajor axis for semimajor axes between $\sim 9\text{ AU}$ and $\sim 100\text{ AU}$. For systems with dust radius $< 9\text{ AU}$, this relationship overestimates the dust mass. Instead, we calculate the mass of a debris ring around EF Cha using

$$M_{dust} \geq \frac{16}{3} \pi \frac{L_{IR}}{L_*} \rho_s R_{dust}^2 < a > \quad (1)$$

(eqn. 4 in Chen & Jura 2001), where ρ_s is the density of an individual grain, L_{IR} is the dust luminosity, and $< a >$ is the average grain radius. Because Chen & Jura (2001) analyzed $\zeta\text{ Lep}$, a star of similar spectral type to EF Cha, we adopt their model for grain size distribution. Assuming $R_{dust} = 4.3\text{ AU}$, $\rho_s = 2.5\text{ g cm}^{-3}$, and $< a > = 3\,\mu\text{m}$, the dust mass is $4.8 \times 10^{22}\text{ g}$ ($\sim 10^{-5} M_{\oplus}$). Grains with $a = 3\,\mu\text{m}$ will radiate approximately as blackbodies at wavelengths shorter than $\sim 2\pi a$ ($\sim 20\,\mu\text{m}$). As may be seen from Figure 1, most of the excess IR emission at EF Cha appears at wavelengths $\lesssim 20\,\mu\text{m}$.

For blackbody grains at $\sim 4.3\text{ AU}$ with, for example, radius $a = 3\,\mu\text{m}$, the Poynting Robertson (P-R) drag time scale¹ is only 8×10^3 years, much less than 10 Myrs. Yet smaller grains with $a < 1.3\,\mu\text{m}$ would be easily blown away by radiation pressure on a much shorter time-scale. Successive collisions among grains can effectively remove dust particles by grinding down large bodies into smaller grains, which then can be blown out. The characteristic collision time (orbital period/ τ) of dust grains at 4.3 AU from this A9 star is $\sim 10^4$ years. Both PR time and collision time were derived assuming no gas was present in the disk. While gas has not been actively searched for in EF Cha, few debris disk systems

¹In the calculation of P-R timescale, $9.7 L_{\odot}$ was used for the stellar luminosity of EF Cha with a bolometric correction of -0.102 (Cox 2000). Absolute visual magnitude of EF Cha is 2.35 based on the Hipparcos distance of 106 pc.

at $\gtrsim 10$ Myr show presence of gas, indicating early dispersal of gas (Pascucci et al. 2006). A possibility of an optically thin gas disk surviving around a ~ 10 Myr system was investigated by Takeuchi & Artymowicz (2001). However their model of gas disk is pertinent to cool dust at large distances ($\gtrsim 120$ AU), but not to warm dust close to the central star as in EF Cha. In addition, a recent study of OB associations shows that the lifetime of a primordial inner disk is $\lesssim 3$ Myr for Herbig Ae/Be stars (Hernández et al. 2005). Based on the very short time scales of dust grain removal, essentially all grains responsible for significant excess emission at EF Cha in the mid-IR are, therefore, likely to be second generation, not a remnant of primordial dust.

5.2. Debris Disk Systems in the TPZ during the Epoch of Planet Formation

The presence of hot dust has been recognized around other ~ 10 Myr stars, for example, TW Hya, HD 98800, & Hen 3-600 in the TW Hydrae Association. Interesting characteristics of these systems are their large τ ($\gtrsim 10^{-2}$) and late-K and M spectral types. TW Hya and Hen 3-600 show flat IR SED up to $160\mu\text{m}$ consistent with active accretion in their disks (Low et al. 2005). Combined with the presence of substantial gas emission lines from TW Hya, the observed infrared excess emission, at least for these two stars, appears to arise from gaseous dusty disks left over from the protostellar environment. On the other hand, a lack of gas emission (Dent et al. 2005) and the quadruple nature of the HD 98800 system has invoked a flared debris disk as an alternative explanation for its large infrared excess emission (Furland et al. 2007). Many young stars come in multiple systems. However, they hardly display such a high τ as that of HD 98800. Thus, the dust disk around HD 98800 might be an unusual transient phenomenon such that it still contains a dust population composed of a mixture of primordial grains and replenished debris. Some stars display a mixture of warm and cold grains where the overall infrared excess emissions is dominated by the cold dust. Table 1 summarizes the currently known disk systems with warm dust regardless of spectral type and the presence of cold excess or remnant primordial dust at $\sim 8 - 30$ Myr.

What separates EF Cha from the stars described in the previous paragraph is that most of the infrared excess emission, if not all, arises from warm dust in the TPZ, and as described in §5.1, these grains are, clearly, not a remnant of the protostellar disk. Recent Spitzer MIPS observation shows null detection of EF Cha at $70\mu\text{m}$ band, leaving the presence of substantial cold dust unlikely (See Figure 1). This result is consistent with the recent Spitzer observations of other similar Table 1 early-type warm excess systems (η Tel, HD 3003, HD 172555 and HD 113766) in which cold dust from a region analogous to the Sun’s Kuiper belt objects is missing (Chen et al. 2006; Smith et al. 2006). In the following discussion, we

characterize warm excess stars as those with warm dust in the TPZ only and without cold excess (i.e., we exclude stars like β Pictoris).

The fact that all currently known warm excess stars at ages between 8 – 30 Myr belong to nearby stellar moving groups offers an excellent opportunity to address how frequently warm excess emission appears among young stars in the solar neighborhood. Zuckerman & Song (2004) list suggested members of stellar moving groups and clusters (i.e., η Cha cluster, TW Hydra Association, β Pictoris Moving Group, Cha-Near Moving Group, and Tucana/Horologium Association) at ages 8 – 30 Myr, within 100 pc of Earth. Currently Spitzer MIPS archive data are available for all 18 members of the η Cha cluster, all 24 members of TWA, all 52 members of Tucana/Horologium, 25 out of 27 β Pic Moving Group, and 9 out of 19 members of Cha-Near Moving Group. Multiple systems were counted as one object unless resolved by Spitzer. For example, in the β Pictoris Moving Group, HD 155555A, HD 155555B & HD 155555C were counted as a single object; however, HIP 10679 & HIP 10680 were counted as two objects.

Table 1 shows that the characteristics of dust grains depend on the spectral type of the central star. All six warm debris disks considered in this paper harbor early-type central stars (earlier than F3). However, late-type stars in Table 1 (for example, PDS 66, a K1V star from LCC) sometimes show characteristics of T Tauri-like disk excess (i.g., $\tau > 10^{-2}$, flat IR SED, etc.) even at $\gtrsim 10$ Myr (Silverstone et al. 2006). Such apparent spectral dependency perhaps arises from the relatively young ages (~ 10 Myr) of these systems in which late-type stars still possess grains mixed with primordial dust due to a longer dust removal time scale (Hernández et al. 2005). In the above-mentioned five nearby stellar moving groups, 38 out of 129² stars with Spitzer MIPS measurements have spectral types earlier than G0. Therefore, we find $\sim 13\%$ (5/38) occurrence rate for the warm excess phenomenon among the stars with spectral types earlier than G0 in the nearby stellar groups at 8 – 30 Myr. (Beta Pic is the only early-type star among the remaining 33 which has both warm and cold dust.) For LCC, at least one (HD 113766) out of 20 early-type members is a warm excess star giving 5%

²128 stars with Spitzer data plus EF Cha. EF Cha, which appeared in Mamajek et al. (2000), was inadvertently omitted from the suggested members of Cha-Near Moving Group by Zuckerman & Song (2004), but its membership is included in Zuckerman et al. (2007, in prep.). Since the warm excess in EF Cha was found by MSX & IRAS surveys less-sensitive than *Spitzer* MIPS, the addition of EF Cha to the homogenous pool of MIPS surveyed stars does not increase the warm excess occurrence rate inappropriately because MIPS would have easily detected it. In the near future, even if new members are added to these nearby stellar associations, we believe the overall occurrence rate would remain similar to the current estimate because most A- through early-M type members of these stellar associations, excepting perhaps the Cha-Near Moving Group, are already well established through extensive searches and almost all the members are already surveyed by *Spitzer* MIPS.

frequency (see Table 1 & 2 in Chen et al. 2005). This rate can reach a maximum of 30% when we take into account five early-type LCC members that show excess emission at $24\mu\text{m}$ but have only upper-limit measurements at MIPS $70\mu\text{m}$ band. G0 type was chosen to separate the two apparently different populations because no G-type star except T Cha appears in Table 1. Furthermore, the spectral type of T Cha is not well established (G2-G8) and it may be a K-type star like other K/M stars in Table 1. Rhee et al. (2007, in preparation) analyze all spectral types in the young nearby moving groups and conclude that the warm excess phenomenon with $\tau \gtrsim 10^{-4}$ occurs for between 4 and 7%; this uncertainty arises because some stars have only upper limits to their $70\mu\text{m}$ fluxes.

We thank Aigen Li for helpful advice and the referee for constructive comments that improved the paper. This research was supported by NASA grant NAG5-13067 to Gemini Observatory, a NASA grant to UCLA, and Spitzer GO program #3600. Based on observations obtained at the Gemini Observatory, which is operated by the Association of Universities for Research in Astronomy, Inc., under a cooperative agreement with the NSF on behalf of the Gemini partnership: the National Science Foundation (United States), the Particle Physics and Astronomy Research Council (United Kingdom), the National Research Council (Canada), CONICYT (Chile), the Australian Research Council (Australia), CNPq (Brazil) and CONICET (Argentina). This research has made use of the VizieR catalogue access tool, CDS, Strasbourg, France and of data products from the Two Micron All Sky Survey (The latter is a joint project of the University of Massachusetts and the Infrared Processing and Analysis Center/California Institute of Technology, funded by the National Aeronautics and Space Administration and the National Science Foundation).

REFERENCES

- Acke, B., & van den Ancker, M. E. 2004, A&A, 426, 151
- Beichman, C. A., et al. 2005, ApJ, 626, 1061
- Beichman, C. A., et al. 2006, ApJ, 639, 1166
- Bryden, G. et al. 2006, ApJ, 636, 1098
- Chen, C. H., & Jura, M. 2001, ApJ, 560, L171
- Chen, C. H., Jura, M., Gordon, K. D., & Blaylock, M. 2005, ApJ, 623, 493
- Chen, C. H., et al. 2006, ApJS, 166, 351

- Clarke, A. J., Oudmaijer, R. D., & Lumsden, S. L. 2005, *MNRAS*, 363, 1111
- Cox, A. N. 2000, *Allen’s Astrophysical Quantities*, 4th ed. Edited by Arthur N. Cox. Publisher: New York: AIP Press; Springer, 2000. ISBN: 0387987460
- Dent, W. R. F., Greaves, J. S., & Coulson, I. M. 2005, *MNRAS*, 359, 663
- Dommanget, J., & Nys, O. 1994, *Communications de l’Observatoire Royal de Belgique*, 115, 1
- Egan, M. P., et al. 2003, *VizieR Online Data Catalog*, 5114, 0
- Furland et al. 2007, *ApJ* in press, astro-ph/07050380.
- Gorlova N., et al. 2004, *ApJS*, 154, 448
- Gorlova, N., Rieke, G. H., Muzerolle, J., Stauffer, J. R., Siegler, N., Young, E. T., & Stansberry, J. H. 2006, *ApJ*, 649, 1028
- Hauschildt, P. H., Allard, F., & Baron, E. 1999, *ApJ*, 512, 377
- Hernández, J., Calvet, N., Hartmann, L., Briceño, C., Sicilia-Aguilar, A., & Berlind, P. 2005, *AJ*, 129, 856
- Hines, D. C. et al. 2006, *ApJ*, 638, 1070
- Kessler-Silacci, J., et al. 2006, *ApJ*, 639, 275
- Lisse, C. M., Beichman, C. A., Bryden, G., & Wyatt, M. C. 2007, *ApJ*, 658, 584
- Low, F., Smith, P. S., Werner, M., Chen, C., Krause, V., Jura, M., & Hines, D. C. 2005, *ApJ* 631, 1170
- Luhman, K. L., & Steeghs, D. 2004, *ApJ*, 609, 917
- Mamajek, E. M, Lawson, W. A., & Feigelson, E. D. 1999, *ApJ*, 516, L77
- Mamajek, E. E., Lawson, W. A., & Feigelson, E. D. 2000, *ApJ*, 544, 356
- Mamajek, E. E., Meyer, M. R., & Liebert, J. 2002, *AJ*, 124, 1670
- Megeath, S. T., Hartmann, L., Luhman, K. L., & Fazio, G. G. 2005, *ApJ*, 634, L113
- Pascucci, I., et al. 2006, *ApJ*, 651, 1177
- Rhee, J. H., & Larkin, J. E. 2006, *ApJ*, 640, 625

- Rhee, J. H., Song, I., Zuckerman, B., & McElwain, M. 2007, *ApJ*, 660, 1556
- Rieke, G. H., et al. 2005, *ApJ*, 620, 1010
- Schuetz, O., Meeus, G., & Sterzik, M. F. 2005, *A&A*, 431, 175
- Silverstone, M. D. et al. 2006, *ApJ*, 639, 1138
- Smith, P. S., Hines, D. C., Low, F. J., Gehrz, R. D., Polomski, E. F., & Woodward, C. E. 2006, *ApJ*, 644, L125
- Song, I., Zuckerman, B., Weinberger, A. J., Becklin, E. E. 2005, *Nature*, 436, 363
- Song, I., Zuckerman, B., Bessell, M. 2007, submitted to *ApJ*.
- Su, K. Y. L., et al. 2005, *ApJ*, 628, 487
- Takeuchi, T., & Artymowicz, P. 2001, *ApJ*, 557, 990
- Wyatt, M. C., Smith, R., Greaves, J. S., Beichman, C. A., Bryden, G., & Lisse, C. M. 2007, *ApJ*, 658, 569
- Zuckerman, B., Song, I., Bessell, M. S., & Webb, R. A. 2001, *ApJ*, 562, L87
- Zuckerman, B., Song, I., & Webb, R. A. 2001, *ApJ*, 559, 388
- Zuckerman, B., & Song, I. 2004, *ARA&A*, 42, 685
- Zuckerman, B., Song, I., Weinberger, A., Bessell, M. 2007 *ApJ* Letter in preparation.

Table 1. Debris systems in the terrestrial planetary zone in the epoch of terrestrial planet formation

Star (1)	Sp. Type (2)	V (mag) (3)	D (pc) (4)	R_{star}^a (R_{\odot}) (5)	T_{star} (K) (6)	T_{dust} (K) (7)	τ ($\times 10^{-4}$) (9)	age (Myr) (10)	Warm excess Only (11)	Disk Characteristics (12)	Membership (13)	References (14)
η Cha	B8 ^b	5.5	97	2.37	11000	320	1.5	8	Yes	Debris	η Cha	1
EF Cha	A9	7.5	106	1.92	7400	240	10	10	Yes	Debris	Cha-Near	2
HD 113766	F3V	7.5	131	... ^c	7000	350	150	10 ^d	Yes	Debris	LCC	3,5,6
HD 172555	A7V	4.8	29	1.52	8000	320	8.1	12	Yes	Debris	β Pic	3,4,6
η Tel	A0V	5.0	48	1.61	9600	150	2.1	12	Yes	Debris	β Pic	3,6
HD 3003	A0V	5.1	46	1.59	9600	200	0.92	30	Yes	Debris	Tucana/Horologium	7,8
β Pic	A5V	3.9	19	1.37	8600	110 ^e	26	12	No	Debris	β Pic	4
HD 98800	K5Ve	9.1	47	... ^c	4200	160	1100	8	No	Primordial/Debris	TWA	2,7
TW Hya	K8Ve	11.1	56	1.11	4000	150?	>2200	8	No	Primordial/Debris	TWA	2,7
Hen 3-600	M3	12.1	42 ^f	... ^c	3200	250	1000	8	No	Primordial/Debris	TWA	2,7
EP Cha	K5.5 ^b	11.2	97	1.39	4200 ^b	... ^g	>1300 ^g	8	No	Primordial/Debris	η Cha	10,11
ECHA J0843.3-7905	M3.25 ^b	14.0	97	0.87	3400 ^b	... ^g	>2000 ^g	8	No	Primordial/Debris	η Cha	10,11
EK Cha	M4 ^b	15.2	97	0.79	3300 ^b	... ^g	>590 ^g	8	No	Primordial/Debris	η Cha	10,11
EN Cha	M4.5 ^b	15.0	97	... ^c	3200 ^b	... ^g	>480 ^g	8	No	Primordial/Debris	η Cha	10,11
ECHA J0841.5-7853	M4.75 ^b	14.4	97	0.51	3200 ^b	... ^g	>480 ^g	8	No	Primordial/Debris	η Cha	10,11
ECHA J0844.2-7833	M5.75 ^b	18.4	97	0.40	3000 ^b	... ^g	>400 ^g	8	No	Primordial/Debris	η Cha	10,11
T Cha	G2-G8	11.9	66	... ^h	... ^h	... ^h	... ^h	10	No	Primordial/Debris	Cha-Near	7,12
PDS 66	K1Ve	10.3	~85	1.35 ⁱ	4400	... ^g	>2200 ^g	10 ^d	No	Primordial/Debris	LCC	6,9

^aEstimated using a total integrated flux for a given distance (col. 4) assuming that each star is a single object.

^bFrom Luhman & Steeghs (2004)

^cMultiple systems: HD 113766 (binary), HD 98800 (quadruple), Hen 3-600 (triple), & EN Cha (binary) from Zuckerman & Song (2004).

^dMamajek et al. (2002) estimate the age of LCC at ~16 Myr. However, Song et al. (2007) report a younger age of ~10 Myr.

^eBased on the single temperature blackbody fit to the dominant cold excess. However, additional warm excess emission exists above the 110K model fit, indicating the presence of warm disk in terrestrial planetary zone.

^fEstimated photometric distance from Zuckerman & Song (2004)

^gThis lower limit τ is estimated from our two-temperature dust component fit to the infrared excess emission. No dust temperature is given because its IR excess emission cannot be fit with a single temperature blackbody. However, a significant excess emission at mid-IR wavelengths exists which is not the Wien tail of emission from cold dust grains.

^hNo SED fitting was attempted to estimate stellar radius & temperature as well as dust parameters.

ⁱBased on the distance of 85 pc (Silverstone et al. 2006) from Earth

Note. — R_{star} and T_{star} were obtained by fitting the observed optical and near-IR measurements with NextGen stellar atmosphere model (Hauschildt et al. 1999). T_{dust} and τ were estimated by fitting blackbody curves to the infrared excess emission. References: 1. Mamajek et al. (1999) 2. Zuckerman et al. (2007) 3. Schuetz et al. (2005) 4. Zuckerman et al. (2001) 5. Chen et al. (2005) 6. Chen et al. (2006) 7. Zuckerman & Song (2004) 8. Smith et al. (2006) 9. Silverstone et al. (2006) 10. Mamajek et al. (2002) 11. Megeath et al. (2005) 12. Kessler-Silacci et al. (2006)

Table 2. Mid-IR measurements of EF Cha

Band	Central Wavelength (μm)	Flux Density (mJy)	Adopted Photospheric Flux Density (mJy)	Excess Flux Density (mJy)	Instrument
$8\mu\text{m}$	8.28	167 ± 9	119	48	MSX
N	10.4	164 ± 14	84	80	Gemini/TReCS
N	7.7-12.97	–	–	–	TReCS, $\lambda/\Delta\lambda \approx 100$ spectrum
$12\mu\text{m}$	11.5	152 ± 32	58	94	IRAS
$24\mu\text{m}$	24.0	80 ± 4	14	66	MIPS
$25\mu\text{m}$	23.7	110 ± 21	14	96	IRAS
$70\mu\text{m}$	70.0	$< 22.4^{\text{a}}$	1.7	< 20.7	MIPS

^a 3σ upper limit to the non-detection.

Note. — Both MSX and IRAS flux densities were color-corrected using the method described in Rhee et al. (2007).

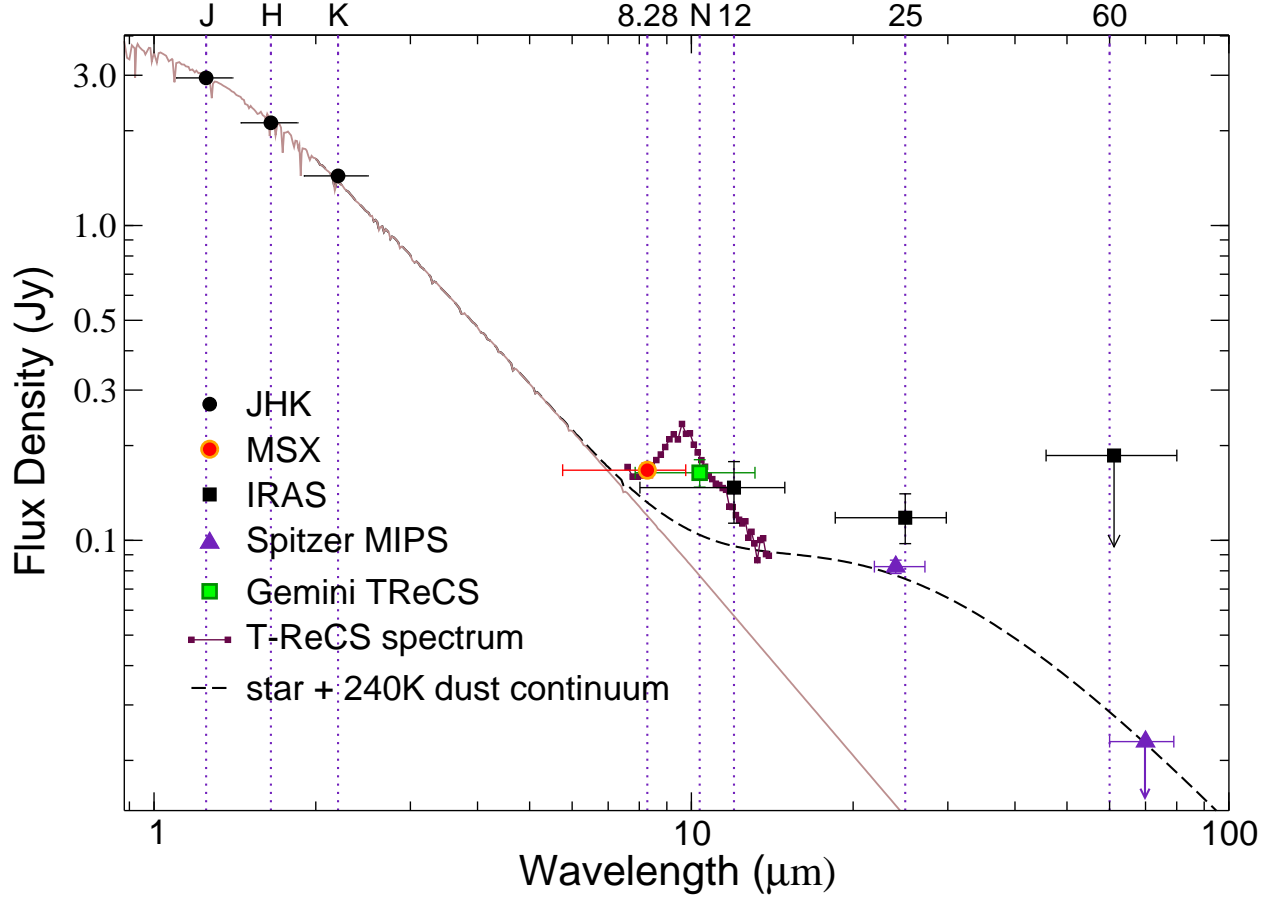


Fig. 1.— Spectral energy distribution of EF Cha created by fitting existing optical and near-IR measurements with a 7400K stellar atmosphere model. After subtracting the stellar photosphere as well as the silicate emission feature near $10\ \mu\text{m}$, the infrared excess continuum emission was fit with a single temperature blackbody model of 240 K. For each measurement, the horizontal bars indicate the passband of the filter used and the vertical bars depict the flux uncertainties. Flux density values for the plotted mid-IR points are given in Table 2.